Review of Catalytic Conditioning of Biomass-Derived Syngas

ARTICLE *in* ENERGY & FUELS · APRIL 2009

Impact Factor: 2.79 · DOI: 10.1021/ef800830n

3 AUTHORS:

Matthew M. Yung
Battelle Memorial Institute
49 PUBLICATIONS **460** CITATIONS
SEE PROFILE

Whitney Jablonski
National Renewable Energy Laboratory
26 PUBLICATIONS **333** CITATIONS
SEE PROFILE

K. A. Magrini-Bair
29 PUBLICATIONS **569** CITATIONS
SEE PROFILE

Reviews

Review of Catalytic Conditioning of Biomass-Derived Syngas

Matthew M. Yung,* Whitney S. Jablonski, and Kimberly A. Magrini-Bair

National Bioenergy Center, National Renewable Energy Laboratory, 1617 Cole Boulevard, Golden, Colorado 80401

Received September 30, 2008. Revised Manuscript Received January 15, 2009

Thermochemical conversion of biomass to create fuels and chemical products may be achieved through the gasification route via syngas. The resulting biomass-derived raw syngas contains the building blocks of carbon monoxide and hydrogen as well as undesired impurities, such as tars, hydrocarbons, hydrogen sulfide, ammonia, hydrogen chloride, and other trace contaminants. These impurities require removal, usually through catalytic conditioning, to produce a quality syngas for end-use synthesis of liquid fuels, such as mixed alcohols and Fischer−Tropsch liquids. In the past decade, significant research attention has been focused on these catalytic processes. This contribution builds on previous reviews and focuses on capturing the work on catalytic conditioning of biomass-derived syngas that have been performed since the Dayton review in 2002, with an emphasis on tar destruction and steam reforming catalysts. This review organizes and discusses the investigations of catalytic conditioning of biomass-derived syngas with various catalyst formulations and also discusses the roles of catalyst additives. Key technical challenges and research areas for the advancement of liquid fuel synthesis via thermochemical conversion of biomass are also discussed.

1. Introduction

The majority of the world's energy is supplied by carbon-based fossil fuels, such as coal, oil, and natural gas. These fossil energy sources are nonrenewable, and their reserves are becoming depleted, which has led to an increased focus on renewable energy sources. One renewable resource currently receiving substantial attention for fuel production is lignocellulosic biomass. The main routes of producing fuels from biomass include (1) gasification to produce syngas, (2) liquefaction and pyrolysis to produce bio-oils, (3) hydrolysis to form aqueous phase sugars or lignin, which can be further processed via fermentation or reforming, and (4) transesterification of triglycerides to produce biodiesel.[1] The focus of this review follows the gasification route to produce useable syngas, which could then be used to synthesize fuels, such as Fischer−Tropsch liquids or mixed alcohols.

The formation of tars during biomass gasification is one of the primary obstacles preventing commercialization of this technology. The definition of "tars" varies, but tars generally comprise the condensable fraction of organic gasification products, largely consisting of aromatic compounds, such as benzene, toluene, and naphthalene.[2−4] Tars can present a number of process challenges, including coking of catalysts and condensation on downstream piping, filters, and other equipment,[3] and the cost of tar removal can be as much as the overall process cost to produce ethanol.[2]

Removing impurities from syngas can be accomplished through several routes, including common physical separation technologies, such as filtration and aqueous or organic liquid scrubbing. Although these unit operations may be effective, they require significant heating and cooling steps unless the gas is needed at near-ambient temperature, and these heat penalties decrease the overall process efficiency. In addition, liquid scrubbing produces large amounts of liquid waste/wastewater that requires downstream treatment and/or recycle. Thermal cracking can remove most of the tars present in syngas, although cracking efficiency improves with temperatures that are significantly higher (>1100 °C) than typical biomass gasification temperatures, which again imposes a heat penalty.[3] Syngas can also be conditioned via catalytic hot gas cleanup. As noted by Dayton, catalytic hot gas cleanup is more efficient than aqueous scrubbing or thermal cracking because it does not create wastewater, can be operated at the same temperature as the gasifier, and improves the carbon efficiency by reforming tars to create more syngas.

Tar cracking consists of several important reactions (e.g., steam reforming, dry reforming, and partial oxidation), which may occur to different extents depending upon reaction conditions. The main products from these reactions are hydrogen, carbon monoxide, short-chain hydrocarbons, such as methane, and oxygenated species, such as methanol (the concentrations of the products depend upon the initial syngas composition). Currently, the two main industrial applications of steam reform-

* To whom correspondence should be addressed. Telephone: +1 (303) 384-7771. Fax: +1 (303) 384-6363. E-mail: matthew_yung@nrel.gov.

(1) Huber, G. W.; Iborra, S.; Corma, A. *Chem. Rev.* **2006**, *106*, 4044.

(2) Milne, T. A.; Abatzoglou, N.; Evans, R. J. Biomass gasification "tars": Their nature, formation and conversion. National Renewable Energy Laboratory (NREL) Technical Report, Golden, CO, 1998; Report NREL/TP 570-25357.

(3) Dayton, D. A review of the literature of catalytic biomass tar destruction. National Renewable Energy Laboratory (NREL) Technical Report, Golden, CO, 2002; Report NREL/TP-510-32815.

(4) Devi, L.; Ptasinski, K. J.; Janssen, F. J. J. G. *Biomass Bioenergy* **2003**, *24*, 125.

10.1021/ef800830n CCC: $40.75
Published on Web 03/11/2009

ing are (1) steam methane reforming (SMR) and (2) naphtha steam reforming, both of which were pioneered by petrochemical companies.[5] The steam reforming reactions usually occur on metal catalysts, most commonly nickel-based.[6] Nickel/alumina (Ni/Al_2O_3) commercial catalysts have been extensively used for tar reforming of biomass-derived syngas. Catalytic tar cracking can be performed either during gasification by placing catalysts directly in the gasification unit or after gasification using a separate, downstream catalytic reactor.

The main limitation for hot gas catalytic tar cracking is catalyst deactivation.[7] Deactivation occurs from both physical and chemical processes associated with the harsh reaction conditions and impurities in the feed stream. Attrition, coking, and sulfur poisoning are the primary deactivation mechanisms that affect the efficient catalytic conditioning of biomass-derived syngas, although the cumulative effects of the other trace inorganic species that are present in biomass (e.g., Si, Al, Ti, Fe, Ca, Mg, Na, K, P, S, and Cl) must also be considered.[8]

2. Basics of Biomass Gasification

Gasification can be used to thermochemically convert solid biomass into a gas-phase mixture of carbon monoxide (CO), hydrogen (H_2), carbon dioxide (CO_2), methane (CH_4), organic vapors, tars (benzene and other aromatic hydrocarbons), water vapor, hydrogen sulfide (H_2S), residual solids, and other trace species (HCN, NH_3, and HCl), depending upon process conditions.[9] Other inorganic materials present in biomass (Si, Al, Ti, Fe, Ca, Mg, Na, K, P, S, and Cl) may also enter the gas phase.[8] Gasification of biomass occurs when it is heated to high temperatures (500−900 °C) in the presence of a gasifying agent, such as air, oxygen, steam, CO_2, or mixtures of these components.[10] The general reaction of biomass gasification is shown in eq 1. The actual composition of the product gas is dependent upon the biomass feedstock, gasification parameters, and gasifying agent. The extent of the partial oxidation of the volatile products governs the composition of the product gas.[3]

$$\begin{aligned}\text{biomass} + \text{oxidant}\,(O_2, H_2O) \rightarrow\ & CO, H_2, CO_2, H_2O, CH_4 + \\ & \text{hydrocarbons} \\ & \rightarrow \text{tar} + \text{char} + \text{ash} \\ & \rightarrow H_2S + HCN + NH_3 + HCl + \text{sulfur species}\end{aligned} \quad (1)$$

The choice of the gasifying agent changes the quality of the syngas that is produced and also affects the syngas suitability for various end-use applications. Three primary types of biomass gasification can be distinguished on the basis of the gasifying agent and the way in which heat is provided for the gasification reactions: directly heated (i) air and (ii) oxygen gasification and (iii) indirectly heated gasification. For the direct processes, the injected gasifying agent burns part of the feedstock to provide the heat required to gasify the remaining feedstock in an air-limited environment. Air gasification produces a syngas rich in nitrogen (50−65%) and low in calorific value (4−8 MJ N^{-1} m^{-3}). Oxygen gasification requires an O_2-producing plant, which increases costs and energy consumption but produces a syngas low in N_2 content and high in calorific value (10−18 MJ N^{-1} m^{-3}). Indirectly heated gasifiers do not require air or O_2 input because the heat required for gasification is generated outside of the gasifier. Indirectly heated gasifiers produce a syngas with a calorific value similar to that of the direct O_2-produced syngas, and steam can be input to enhance gasification reactions.[11] A technoeconomic analysis by Tijmensen et al.[12] showed that pressurized air or O_2 biomass gasification may become more economical with large-scale systems.

An ongoing technoeconomic analysis at the National Renewable Energy Laboratory (NREL), comparing direct oxygen to indirect steam biomass gasification for ethanol synthesis, indicates that the addition of an air separation unit is the biggest additional cost for the O_2-blown case. With downstream operations held constant, an ASPEN-based model estimated the cost of ethanol production from a 2000 dry U.S. tons of biomass per day plant using an atmospheric steam blown gasifier at $1.01/gallon,[13] whereas the cost for pressurized (∼400 psi) O_2 gasification was $1.58/gallon.[14]

Important catalytic reactions in the conversion of biomass to fuels that influence the syngas composition (steam reforming, dry reforming, and water−gas shift) are listed in eqs 2−4. The syngas from air gasification generally consists of a H_2/CO ratio ≤ 1, which is suitable for combustion but ill-suited for fuel synthesis.[15] Steam gasification of biomass produces syngas with a H_2/CO ratio > 1, which is more suitable for synthesis of hydrocarbon fuels or methanol.[15,16] Mixtures of gasifying agents can be used to create intermediate H_2/CO ratios, and additional tuning of the H_2/CO ratio can be achieved through the water−gas shift reaction to tailor syngas for a specific application. Reviews by Wang et al.[10] and Devi et al.[4] provide more detailed discussion of the advances and technical issues associated with biomass gasification for production of fuels and electricity.

$$C_nH_m + nH_2O \rightarrow nCO + (n + m/2)H_2 \quad \text{(steam reforming)} \quad (2)$$

$$C_nH_m + nCO_2 \rightarrow (2n)CO + (m/2)H_2 \quad \text{(dry reforming)} \quad (3)$$

$$CO + H_2O \leftrightarrow CO_2 + H_2 \quad \text{(water−gas shift)} \quad (4)$$

Purification of the product gas is one of the major issues facing thermochemical conversion of biomass to fuels. Tars, other unwanted hydrocarbons, and trace contaminants should be removed or catalytically converted into desired species to protect downstream fuel synthesis catalysts and more efficiently use the biomass carbon and hydrogen content. Catalytic tar reforming provides both of these functions by simultaneously removing unwanted species and generating useable products (e.g., CO, H_2, and CO_2).

3. Catalytic Conditioning Studies

To capture the recent growth and numerous studies in the field of catalytic conditioning of biomass-derived syngas, this review

(5) Rostrup-Nielsen, J. *Catal. Today* **2002**, *71*, 243.
(6) Melo, F.; Morlanes, N. *Catal. Today* **2005**, *107−108*, 458.
(7) Sehested, J. *Catal. Today* **2006**, *111*, 103.
(8) Bain, R. L.; Dayton, D. C.; Carpenter, D. L.; Czernik, S. R.; Feik, C. J.; French, R. J.; Magrini-Bair, K. A.; Phillips, S. D. *Ind. Eng. Chem. Res.* **2005**, *44*, 7945.
(9) Turn, S. Q.; Bain, R. L.; Kinoshita, C. M. *Int. Sugar J.* **2002**, *104*, 268.
(10) Wang, L.; Weller, C. L.; Jones, D. D.; Hanna, M. A. *Biomass Bioenergy* **2008**, *32*, 573.
(11) Bauen, A. *Encycl. Energy* **2004**, *1*, 213.
(12) Tijmensen, M. J. A.; Faaij, A. D.; Hamelinck, C. N.; van Hardeveld, M. R. M. *Biomass Bioenergy* **2002**, *23*, 129.
(13) Phillips, S.; Aden, A.; Jechura, J.; Dayton, D.; Eggeman, T. Thermochemical ethanol via indirect gasification and mixed alcohol synthesis of lignocellulosic biomass. National Renewable Energy Laboratory (NREL) Technical Report, Golden, CO, 2007; Report NREL/TP-510-41168.
(14) Dutta, A.; Phillips, S. Thermochemical ethanol via direct gasification and mixed alcohol synthesis of lignocellulosic biomass. Draft of National Renewable Energy Laboratory (NREL) Technical Report, Golden, CO, 2009.
(15) Torres, W.; Pansare, S. S.; Goodwin, J. G. *Cat. Rev.* **2007**, *49*, 407.
(16) Gil, J.; Corella, J.; Aznar, M. P.; Caballero, M. A. *Biomass Bioenergy* **1999**, *17*, 389.

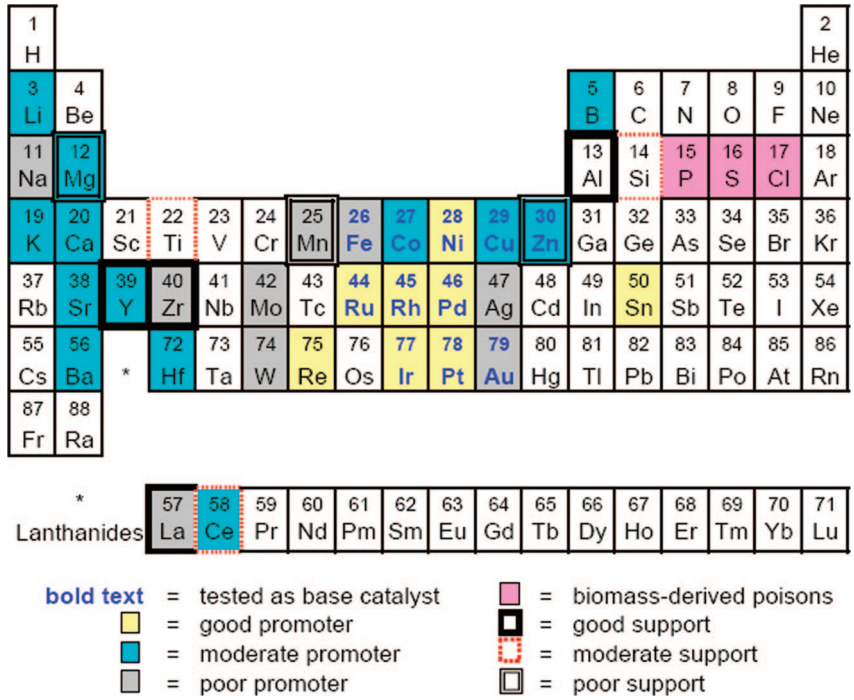

Figure 1. Elements investigated for catalytic conditioning studies.

focuses on the studies that have occurred since the Dayton review in 2002.[3] Many catalysts and promoters/additives, especially Ni-based systems, have been studied for conditioning of biomass-derived syngas, and this review provides the reader with an overview of important findings from this work as well as reference tables detailing these studies, organized by catalyst composition. This review contains studies on catalytic conditioning of (i) syngas obtained from biomass gasification, (ii) modeled syngas compositions, (iii) main constituents of biomass-derived syngas (e.g., methane, ethylene, and benzene), and (iv) model compounds and fuels (e.g., propane, phenol, toluene, ethanol, octane, diesel, and NORPAR-13) that have similar chemistry on catalytic surfaces as syngas constituents. The authors also direct the reader to other excellent reviews by Milne and Evans,[2] Dayton,[3] Devi et al.,[4] Huber et al.,[1] and Torres et al.[15] for additional insight into the work that has been performed on catalytic conditioning of biomass-derived syngas.

The composition of heterogeneous catalysts can be divided into three primary components: (1) an active catalytic phase or metal, (2) a promoter, which increases activity and/or stability, and (3) a high surface area support that facilitates dispersion of the active phase.[17] Recent investigations of catalyst compositions comprising these three primary components and their influence on activity for conditioning biomass-derived syngas are reviewed in the following sections. Figure 1 shows the elements that have been examined for these various functionalities and provides a general representation of how their presence influences the activity of catalysts. In addition to a discussion of catalyst composition within this section, catalyst composition as it pertains to mitigation of catalyst deactivation is also given in Section 4. Catalyst Deactivation. For the reader's reference, Tables 1−3 organize catalysts by composition and show the conditioning reactions that were studied with the various catalyst compositions. Table 1 focuses on non-Ni-based conditioning catalysts. Table 2 shows studies on promoted and unpromoted Ni/Al_2O_3 catalysts. Table 3 organizes the studies on minerals (e.g., olivine and dolomite) and Ni catalysts on supports other than Al_2O_3.

3.1. Base Metal Studies. A variety of metals have been evaluated for conditioning biomass-derived syngas (see Table 1), and the highest reforming activities were achieved with Ni- and Rh-based catalysts. Nickel-based steam reforming catalysts have been widely used commercially in the petrochemical industry for methane and naphtha reforming. These Ni catalysts have also shown activity for tar destruction, hydrocarbon reforming, water−gas shift (WGS), and NH_3 decomposition.[3] Caballero et al. coupled a Ni-based commercial steam reforming catalyst with a dolomite guard bed for hydrocarbon reforming during biomass gasification in the simultaneous presence of steam and O_2.[18] They observed increases in CO and H_2 and decreases in tars, CH_4, and CO_2 as compared to the noncatalyzed case.

Aupretre et al. tested Group VIII metals (except for Os, Co, and Ir) in addition to Fe, Cu, and Zn as base metals supported on Al_2O_3 for ethanol steam reforming at 700 °C.[19] The highest H_2 yields were obtained with Rh and Ni catalysts. To complete the assessment of Group VIII metals, Zhang et al. tested Ir, Co, and Ni for ethanol steam reforming at 700 °C and identified the Ni-based catalysts as the most promising in their study.[20] Tomishige et al. evaluated Rh, Ru, Pt, Pd, and Ni supported on CeO_2-SiO_2 for steam reforming of biomass-derived tars. Using a carbon basis for tar conversion, they found the order of activity to be Rh > Pt > Ni > Pd > Ru.[21] For methane dry reforming, Tsyganok et al.[22] found that the order of activity for metal catalysts supported on periclase $MgAlO_x$ was Ru = Rh = Ir >

(17) Bartholomew, C. H.; Farrauto, R. J. *Fundamentals of Industrial Catalytic Processes*, 2nd ed.; Wiley: New York, 2006.

(18) Caballero, M. A.; Aznar, M. P.; Gil, J.; Martin, J. A.; Frances, E.; Corella, J. *Ind. Eng. Chem. Res.* **1997**, *36*, 5227.

(19) Aupretre, F.; Descorme, C.; Duprez, D. *Catal. Commun.* **2002**, *3*, 263.

(20) Zhang, B.; Tang, X.; Li, Y.; Cai, W.; Xu, Y.; Shen, W. *Catal. Commun.* **2006**, *7*, 367.

(21) Tomishige, K.; Miyazawa, T.; Asadullah, M.; Ito, S.; Kunimori, K. *Green Chem.* **2003**, *5*, 399.

(22) Tsyganok, A.; Inaba, M.; Tsunoda, T.; Hamakawa, S.; Suzuki, K.; Hayakawa, T. *Catal. Commun.* **2003**, *4*, 493.

Table 1. Catalytic Conditioning Studies Using Non-nickel Metals

metal	promoter	support	reaction	conditions	references
Au	Mg	Al_2O_3	dry reforming	800 °C	22
Co		Al_2O_3	EtOH SR	300−500 °C, S/C = 1.5	130
Co		CeO_2	EtOH SR	700 °C, S/C = 1.5	20
Co		MgO	naphthalene SR	900 °C, S/C = 0.6	131, 132
Co		TiO_2	EtOH SR	300−500 °C, S/C = 1.5	130
Co	Cu, Na	ZnO	EtOH SR	300−450 °C, S/C = 6.5	67
Co	Ni, Na	ZnO	EtOH SR	300−450 °C, S/C = 6.5	67
Co		ZrO_2	EtOH SR	300−500 °C, S/C = 1.5	130
Cu		Al_2O_3	EtOH SR	700 °C, S/C = 1.5	19
Fe		Al_2O_3	EtOH SR	700 °C, S/C = 1.5	19
Fe		Al_2O_3	SR of gasified oak	500−700 °C	143
Ir		CeO_2	EtOH SR	700 °C, S/C = 1.5	20
Ir	Mg	Al_2O_3	dry reforming	800 °C	22
Pd		Al_2O_3	EtOH SR	700 °C, S/C = 1.5	19
Pd	Mg	Al_2O_3	dry reforming	800 °C	22
Pd		CeO_2	cellulose gasification	500−550 °C	21
Pd	CeO_2	SiO_2	SR of gasified cedar	600 °C	21
Pt		Al_2O_3	EtOH SR	700 °C, S/C = 1.5	19
Pt	Mg	Al_2O_3	dry reforming	800 °C	22
Pt	Pd	Al_2O_3	diesel and JP8 ATR	400 °C, S/C = 2.5	109
Pt		CeO_2	cellulose gasification	500−550 °C	21
Pt	Pd	CeO_2	diesel and JP8 ATR	400 °C, S/C = 2.5	109
Pt	CeO_2	SiO_2	SR of gasified cedar	600 °C	21
Rh		Al_2O_3	EtOH SR, cellulose gasification	500−700 °C	19, 21
Rh	CeO_2	Al_2O_3	cellulose gasification	500−550 °C	21
Rh	Mg	Al_2O_3	dry reforming	800 °C	21
Rh		CeO_2	cellulose gasification	500−550 °C	21
Rh		CeO_2	phenol SR	575−730 °C	133
Rh	Mg	CeO_2	phenol SR	575−730 °C	133
Rh		MgO	cellulose gasification	500−550 °C	21
Rh		MgO	phenol SR	575−730 °C	133
Rh		SiO_2	cellulose gasification	500−600 °C	21, 60
Rh	CeO_2	SiO_2	cellulose gasification	600 °C	60
Rh	CeO_2	SiO_2	cedar SR, gasification, POX	500−750 °C	21, 145−149
Rh		TiO_2	cellulose gasification	500−550 °C	21
Rh		ZrO_2	phenol SR	575−730 °C	133
Rh	CeO_2	ZrO_2	cellulose gasification	500−550 °C	21
Rh	Mg	ZrO_2	phenol SR	575−730 °C	133
Rh	Mg, CeO_2	ZrO_2	phenol SR	575−730 °C	133
Ru		Al_2O_3	EtOH SR	700 °C, S/C = 1.5	19
Ru	Mg	Al_2O_3	dry reforming	800 °C	22
Ru		CeO_2	cellulose gasification	500−550 °C	21
Ru	CeO_2	SiO_2	SR of gasified cedar	600 °C	21
Zn		Al_2O_3	EtOH SR	700 °C, S/C = 1.5	19

Pt > Pd ≫ Au. From these studies, Rh, Ni, and Pt emerged as the best potential base metals for use in steam reforming catalysts. In addition to activity testing, Tomishige and Tsyganok also collected coking data and found that Rh coked significantly less than most of the other metals tested. While Rh and Pt have shown high reforming activity, their high cost limits their use for large, industrial applications. As a result of the high cost of Rh and Pt, more studies have focused on Ni-based catalysts.

3.2. Support Effects on Nickel Catalysts. *3.2.1. Metal Oxides.* Support materials can provide mechanical strength/integrity, surfaces on which to disperse active catalytic materials, and they may also play a chemical role in catalysis. The support can react with the active metal to form a new phase and also with reactants in the system by providing adsorption sites. The acidity/basicity, surface area, pore structure, and electronic structure of the support can affect the reducibility, metal dispersion, mechanical strength, and the overall nature of the active sites on a catalyst. These parameters influence the activity of the catalyst and can be manipulated for optimal catalyst design. A number of authors have studied the effects of supports on Ni-based catalysts for reforming reactions and selected studies are discussed below.

The most commonly used support for commercial Ni steam reforming catalysts has been alumina (Al_2O_3). Alumina has worked well for natural gas (methane) steam reforming (SMR) catalysts, but biomass-derived syngas contains a wide range of impurities that negatively influence the activity of conventional SMR catalysts. Two approaches to improve the catalytic performance of these materials have included altering the Al_2O_3 by combining it with an additive and switching to an entirely different support. Roh et al.[23] combined a γ-alumina support material obtained from Sasol with 30% MgO. They found that Ni dispersion increased by nearly a factor of 12, constant activity was maintained for 24 h, and the CH_4 conversion for SMR over $Ni/MgO-Al_2O_3$ improved by more than 25% as compared to the nonpromoted Ni/Al_2O_3. Temperature-programmed reduction (TPR) results indicated a strong metal−support interaction in the $Ni-MgO-Al_2O_3$ system, as shown by the high temperatures required to reduce nickel species. Lanthanum oxide was shown to be a promising support and provided high conversions for reforming reactions while showing good resistance to deactivation by carbon deposition.[24,25] Sun et al.[24] studied low-temperature ethanol steam reforming at 250 °C on supported nickel catalysts and found the following order of activity: $Ni/La_2O_3 > Ni/Y_2O_3 > Ni/Al_2O_3$. Another study by Seok et al.[25]

(23) Roh, H.; Koo, K.; Jeong, J.; Seo, Y.; Seo, D.; Seo, Y.; Yoon, W.; Park, S. *Catal. Lett.* **2007**, *117*, 85.

(24) Sun, J.; Qiu, X.; Wu, F.; Zhu, W. *Int. J. Hydrogen Energy* **2005**, *30*, 437.

(25) Seok, S.; Choi, S.; Park, E.; Han, S.; Lee, J. *J. Catal.* **2002**, *209*, 6.

Table 2. Promoted and Unpromoted Ni/Al_2O_3 Conditioning Catalysts

metal	promoter	support	reaction	conditions	references
Ni		Al_2O_3	C_7H_{14} SR	580 °C, S/C = 1	36
Ni		Al_2O_3	C_8H_{18} SR	750 °C, S/C = 3	135
Ni		Al_2O_3	dry reforming	650 °C	25
Ni		Al_2O_3	EtOH SR	320 °C, 700 °C, S/C = 1.5	19, 24
Ni		Al_2O_3	NORPAR-13 SR	515 °C, S/C = 3	66
Ni		Al_2O_3	propane SR	550 °C, S/C = 1.3	136
Ni		Al_2O_3	SMR	420−800 °C	23, 27, 70
Ni		Al_2O_3	SR of gasified cedar	650 °C	31
Ni		Al_2O_3	toluene/naphthalene SR	650−850 °C, S/C ∼ 5	58, 145
Ni	Ag	Al_2O_3	SMR, EtOH SR	420−600 °C, S/C = 1−2	70, 71
Ni	Ba, Mn	Al_2O_3	dry reforming	650 °C	25
Ni	Ca	Al_2O_3	C_8H_{18} SR, POX	700 °C, S/C = 3	68
Ni	Ca, K	Al_2O_3	cedar gasification	700 °C	146
Ni	Ca, Mn	Al_2O_3	dry reforming	650 °C	25
Ni	CeO_2	Al_2O_3	propane SR, EtOH SR	550 °C, S/C = 1−2	72, 136
Ni	CeO_2, MnO	Al_2O_3	dry reforming	650 °C	25
Ni	CeO_2, Rh	Al_2O_3	NORPAR-13 SR	515 °C, S/C = 3	66
Ni	Co	Al_2O_3	toluene SR	650 °C, S/C = 5.7	144
Ni	Co	Al_2O_3	EtOH ATR	550 °C, S/C = 2	72
Ni	Cu	Al_2O_3	EtOH ATR	550 °C, S/C = 2	72
Ni	La	Al_2O_3	dry reforming, propane SR	550−700 °C	79, 136
Ni	La	Al_2O_3	toluene SR	650 °C, S/C = 5.7	144
Ni	Mg	Al_2O_3	EtOH ATR	550 °C, S/C = 2	72
Ni	Mg, Au	Al_2O_3	SMR	550 °C, S/C = 1	69
Ni	Mg, Fe	Al_2O_3	C_8H_{18} SR, POX	700 °C, S/C = 3	68
Ni	Mg, Fe, Co	Al_2O_3	C_8H_{18} SR, POX	700 °C, S/C = 3	68
Ni	Mg, K	Al_2O_3	C_2H_4/benzene, wood SR	700−875 °C, S/C = 3−5	8, 101
Ni	Mg, K, Fe	Al_2O_3	C_8H_{18} SR, POX	700 °C, S/C = 3	68
Ni	Mg, K, Fe	Al_2O_3	SMR	700−800 °C, S/C ∼ 2	23, 63
Ni	Mg, La, Ru	Al_2O_3	C_7H_8O SR	750 °C	140
Ni	Mg, Mn	Al_2O_3	dry reforming	650 °C	24
Ni	Mg, Ru	Al_2O_3	SMR	700 °C, S/C = 2	60, 61
Ni	Mn	Al_2O_3	dry reforming	650 °C	25
Ni	Mn, K	Al_2O_3	dry reforming	650 °C	25
Ni	Mn, Na	Al_2O_3	dry reforming	650 °C	25
Ni	Pd	Al_2O_3	octane, SMR	750−850 °C, S/C ∼ 3	36, 135
Ni	Pt	Al_2O_3	SMR, POX	850 °C, S/C ∼ 1	137
Ni	Rh	Al_2O_3	SMR	850 °C	65
Ni	Ru	Al_2O_3	SMR	700 °C, S/C = 2	61
Ni	SiO_2	Al_2O_3	C_7H_{14} SR	580 °C, S/C = 1	36
Ni	SiO_2, Ca, K	Al_2O_3	SR of gasified seed corn	740−820 °C, S/C = 2.8	141
Ni	SiO_2, Mg, K, Fe	Al_2O_3	SR of gasified seed corn	740−820 °C, S/C = 2.8	141
Ni	Yb	Al_2O_3	propane SR	550 °C, S/C = 1.3	136
Ni	Zn	Al_2O_3	EtOH ATR	550 °C, S/C = 2	72

examined Ni on five supports for methane dry reforming at 650 °C. They observed the highest CO_2 conversion on the Al_2O_3-supported catalyst and the following order of activity: Ni/Al_2O_3 > Ni/ZrO_2 > Ni/CeO_2 > Ni/La_2O_3 > Ni/MnO and $Ni/MnAl_2O_4$. While the Ni/Al_2O_3 catalyst showed the highest initial activity, significant coking caused the reactor to plug after several hours of operation, which did not occur with the La_2O_3 catalyst. For the dry reforming of methane at 800 °C, Verykios et al.[26] found that La_2O_3 had higher stability and activity than Al_2O_3 and CaO supports. Postreaction X-ray diffraction (XRD) and X-ray photoelectron spectroscopy (XPS) analysis indicated that, while CH_4 activates on surface Ni crystallites, CO_2 selectively adsorbs onto La_2O_3 to create $La_2O_2CO_3$. The authors attribute the high activity and resistance to deactivation of the La_2O_3 support to the formation of this carbonate species.

Matsumura et al.[27] studied methane steam reforming (SMR) on Ni/Al_2O_3, Ni/SiO_2, and Ni/ZrO_2 and found the highest CH_4 conversion and least coking on the ZrO_2 support. They additionally found that, at 500 °C, steam gradually oxidized Ni to NiO on Ni/Al_2O_3 and Ni/SiO_2, causing catalyst deactivation. Higher temperatures were required for Ni reduction on ZrO_2 than on SiO_2 and Al_2O_3, indicating a strong metal support interaction on the Ni/ZrO_2 catalyst. Other studies have focused on nanocrystalline Ni/ZrO_2 catalysts, in which the ZrO_2 crystallites are smaller than those in conventional ZrO_2 supports, for steam and dry reforming of methane.[28−30] In these studies, the activity levels and coking resistance of the nanocomposite materials were compared to and found to be higher than those on conventional Ni/Al_2O_3 and Ni/ZrO_2catalysts.

Rather than using model tar compounds, Miyazawa et al.[31] evaluated catalysts for steam reforming cedar-derived syngas. They examined several metal oxide supports and found the relative tar destruction activity at 650 °C to be Ni/Al_2O_3 > Ni/ZrO_2 > Ni/TiO_2 > Ni/CeO_2 > Ni/MgO. In this study, the authors propose that the support does not actively participate in reforming or partial oxidation but serves to enhance Ni dispersion.

Hennings et al.[32] investigated different levels of gadolinium-doped ceria as a support for steam reforming of natural gas. TPR studies showed that Gd addition to CeO_2 suppresses reduction at high temperature, leads to higher surface reactivity

(26) Verykios, X. *Int. J. Hydrogen Energy* **2003**, *28*, 1045.
(27) Matsumura, Y.; Nakamori, T. *Appl. Catal., A* **2004**, *258*, 107.
(28) Rezaei, M.; Alavi, S.; Sahebdelfar, S.; Yan, Z.-F. *Energy Fuels* **2006**, *20*, 923.
(29) Rezaei, M.; Alavi, S.; Sahebdelfar, S.; Xinmei, L.; Qian, L.; Yan, Z.-F. *Energy Fuels* **2007**, *21*, 581.
(30) Zhang, Q.; Li, Y.; Xu, B. *Catal. Today* **2004**, *98*, 601.
(31) Miyazawa, T.; Kimura, T.; Nishikawa, J.; Kado, S.; Kunimori, K.; Tomishige, K. *Catal. Today* **2006**, *115*, 254.
(32) Hennings, U.; Reimert, R. *Appl. Catal., A* **2007**, *325*, 41.

Table 3. Metal-Oxide-, Mineral-, and Zeolite-Supported Conditioning Catalysts

metal	promoter	support	reaction	conditions	references
Ni		CeO_2	EtOH SR	700 °C, S/C = 1.5	20
Ni		CeO_2	SMR	800 °C	23
Ni		CeO_2	dry reforming	650 °C	25
Ni		CeO_2	SR of gasified cedar	650 °C	31
Ni		CeO_2	CH_4 POX	700 °C	37
Ni		CeO_2	cellulose gasification	500−600 °C	21, 60
Ni	Pt	CeO_2	diesel and JP8 ATR	400 °C, S/C = 2.5	109
Ni		dolomite	toluene/naphthalene SR	730−850 °C, S/C = 5	58
Ni		dolomite	naphthalene SR	700 °C	139, 142
		dolomite	SR of gasified beech	800−900 °C	138
		dolomite	pine, olive oil gasification	700−900 °C, S/C ∼ 1−6	40, 134
		dolomite	almond shell gasification	770 °C	45
		dolomite	cedar gasification	700 °C	146
Ni		olivine	benzene/toluene SR	830 °C, S/C = 5	55
Ni		olivine	C_2H_4, MeOH SR	750 °C, S/C ∼ 4	42
Ni		olivine	methane/naphthalene SR	800−900 °C, S/C ∼ 4	49
Ni		olivine	SR of gasified wood	850 °C	54
Ni		olivine	pine, olive oil gasification	850 °C, S/C ∼ 1−6	40
Ni		olivine	toluene SR	800 °C	52, 53
Ni		olivine	toluene, SMR	800 °C	47, 57
Ni	CeO_2	olivine	benzene/toluene SR	830 °C, S/C = 5	55
		olivine	SR of gasified beech	800−900 °C	138
		olivine	C_2H_4, MeOH SR	750 °C, S/C ∼ 4	42
		olivine	CH_4, C_7H_8, $C_{10}H_8$ SR	750−900 °C	41
		olivine	methane/naphthalene SR	800−900 °C, S/C ∼ 4	49
		olivine	pine, olive oil gasification	850 °C, S/C ∼ 1−6	40
		olivine	almond shell gasification	700−820 °C	45
		olivine	toluene, SMR	800 °C	47, 57
		sand	SR of gasified beech	800−900 °C	138
		sand	almond shell gasification	770 °C	45
$LaNi_{0.3}Fe_{0.7}O_3$		perovskite	almond shell gasification	600−800 °C	83
Ni		La_2O_3	EtOH SR	320 °C, S/C = 1.5	24
Ni		La_2O_3	dry reforming	650 °C	25
Ni		MgO	SR of gasified cedar	650 °C	31
Ni		MgO	naphthalene SR	900 °C, S/C = 0.6	131, 132
Ni	K	MgO	EtOH SR	650 °C, S/C = 2.1	78
Ni	Li	MgO	EtOH SR	650 °C, S/C = 2.1	78
Ni	Na	MgO	EtOH SR	650 °C, S/C = 2.1	78
Ni		MnO	dry reforming	650 °C	25
Ni		SiO_2	SMR	500 °C	27
Ni		SiO_2	toluene/naphthalene SR	730−850 °C, S/C = 5	58
Ni		SiO_2	cellulose gasification	600 °C	60
Ni	CeO_2	SiO_2	SR of gasified cedar	600 °C	21
Ni	SrO	SiO_2	CH_4 POX, dry reforming	750 °C	150
Ni		TiO_2	SR of gasified cedar	650 °C	31
Ni		Y_2O_3	EtOH SR	320 °C, S/C = 1.5	24
Ni		YSZ	CH_4, C_3H_8, C_8H_{18} SR	800 °C, S/C = 0.5	81, 82
Ni	Sn	YSZ	CH_4, C_3H_8, C_8H_{18} SR	800 °C, S/C = 0.5	81, 82
Ni	SrO	YSZ	CH_4, C_2H_6, C_2H_4 SR	400−1000 °C	151
Ni		ZrO_2	SMR	800 °C	23
Ni		ZrO_2	dry reforming	650 °C	25
Ni		ZrO_2	SR of gasified cedar	650 °C	31
Ni		ZrO_2	SMR	500 °C	27
Ni		ZrO_2	CH_4 POX	700 °C	37
Ni		ZrO_2	dry reforming	650 °C	25
Ni		ZrO_2	cellulose gasification	600 °C	60
Ni	CeO_2	ZrO_2	CH_4 POX	700 °C	37
Ni	CeO_2	ZSM-5	C_7H_{14} SR	580 °C, S/C = 1	36
Ni		H−mordenite	cellulose gasification	600 °C	60
Ni	CeO_2	H−mordenite	cellulose gasification	600 °C	60
Ni		H−ZSM-5	cellulose gasification	600 °C	60
Ni	CeO_2	H−ZSM-5	cellulose gasification	600 °C	60
Ni		H-β	cellulose gasification	600 °C	60
Ni		USY	cellulose gasification	600 °C	60
Ni		Na−mordenite	cellulose gasification	600 °C	60
Ni		Na−Y	cellulose gasification	600 °C	60
Ni		Na−ZSM-5	cellulose gasification	600 °C	60

and oxygen exchange capacity, and reduces the overall oxygen storage capacity as compared to pure CeO_2. They suggest that these Gd−CeO_2 materials could be used as a support in steam reforming to help enhance carbon gasification, thereby preventing deactivation caused by coking.

Zeolites are an important class of crystalline aluminosilicates, which have been widely used in heterogeneous catalysis because of their well-defined pore structures and capabilities of extremely high surface area and surface acidity. The zeolite ZSM-5 is a versatile material that has been used for a variety of heterogeneous catalytic reactions, including catalytic cracking and NO_x-selective catalytic reduction.[33−35] Wang et al.[36] studied ZSM-5 zeolites promoted with CeO_2 as support materials and found that they were effective for tar destruction. They loaded 5 wt

% Ni onto CeO_2-coated ZSM-5 and found that, for C_7H_{14} reforming at 580 °C, the order of activity was Ni/CeZSM-5 > Ni/HZSM-5 ≫ Ni/Al_2O_3. In the presence of 20 ppm H_2S, the Ni/CeZSM-5 catalyst showed high hydrocarbon conversion, which could be further increased by doping with Re to create a Ni/Re/CeZSM-5 catalyst. Xu et al.[37] compared Ni/CeO_2, Ni/ZrO_2, and Ni/CeO_2-ZrO_2 mixed oxide catalysts for methane partial oxidation at 700 °C and found higher activity and coke resistance on the composite supports as compared to the individual metal oxides. For dry methane reforming at 800 °C, however, Potdar et al.[38] found that, while 30 wt % Ni on CeO_2-ZrO_2 showed high initial activity (>95% CH_4 conversion), it quickly deactivated and lost substantial activity after 15 h on stream.

Choudhary et al.[39] studied SMR and methane autothermal reforming (ATR) over $NiCoMgO_x$ and $NiCoMgCeO_x$ supported on ZrO_2-HfO_2. Both catalysts showed high methane conversion during the methane partial oxidation reaction. In the presence of steam and CO_2, however, the $NiCoMgCeO_x$ catalyst performed better than the $NiCoMgO_x$ catalyst, which was attributed to high lattice oxygen mobility because of Ce addition, making it more suitable for methane ATR. They also found that high calcination temperatures could lead to deactivation through the formation of inactive mixed metal oxides. The addition of HfO_2 helped to stabilize the materials that underwent high calcination temperatures (>1200 °C). The catalysts containing MgO showed high methane conversion and selectivity toward CO and H_2.

3.2.2. Dolomite, Olivine, and Other In-Bed Gasification Catalysts. Natural materials, such as dolomite and olivine, have received significant attention for use as tar cracking catalysts.[3,40−42] Dolomite and olivine are inexpensive, readily available, possess good tar reforming activity, and can also adjust syngas composition through water−gas shift and dry reforming reactions.[3,41,43] Dolomite catalysts, having the general formula of $CaCO_3-MgCO_3$, show poor activity for reforming light hydrocarbons, such as methane, and also suffer from poor attrition resistance. This attrition leads to unwanted particulates in the product stream and results in the need for frequent catalyst replacement.[44] Consequently, dolomite is better suited for use in a guard bed reactor (downstream from the gasifier but upstream from the fluidized reforming reactor) to reform tars, as opposed to being located within a fluidized gasification reactor.

Olivine, although not as prevalent as dolomite, is another inexpensive support material that is more attrition-resistant than dolomite and thus more suitable for fluidized-bed operations.[3,41,44] Naturally occurring olivine is a silicate material that also contains mainly Mg and Fe, although other metals (e.g., Mn, Cr, Co, and Ni) may be found in trace amounts or synthetically incorporated.[41] Similar to dolomite, olivine also possesses good tar reforming activity but poor activity for reforming light hydrocarbons, such as methane.[40,45,46] Olivine has been studied for reducing tar formation during biomass gasification[45] and also for naphthalene, toluene, and methane steam reforming, as well as dry methane reforming.[46,47] Olivine has been used as an in-bed additive in fluidized-bed reactors for tar reduction during steam gasification of almond shells[45] and air gasification of a mixture of pine wood chips and olive oil.[40] It has also been employed in a secondary reactor to reduce tars formed from beech-wood-derived syngas.[48] Kuhn et al. measured tar destruction on natural olivine catalysts and found that the geographic origin of the mineral had an influence on the activity.[41] A broad range of tar reforming activity has been reported for olivine catalysts, likely because of a variety of pretreatments and variation in naturally occurring amounts and phases of elements, such as Fe, which have been shown to strongly influence reforming activity.[41]

Corella et al.[40] completed a comparative study between olivine and dolomite as in-bed additives for biomass gasification of olive oil residue and small pine wood chips. They reported that dolomite is ∼1.4 times more effective than olivine for tar conversion, but it created 4−6 times more particulates. For these reasons, it is difficult to definitively say if dolomite or olivine is superior as an in-bed additive, although many researchers agree that neither material is sufficient to achieve the desired level of syngas conditioning.

To improve the steam reforming activity of tars and light hydrocarbons, such as methane, researchers have looked at synthetically incorporating metals, such as nickel, into natural olivine and dolomite.[42,46,49] Courson et al. were among the first to report high methane conversion for steam and dry reforming over impregnated Ni−olivine catalysts.[46] The group explored Ni−olivine catalysts for several studies of importance to reform biomass-derived syngas, including methane steam reforming,[46,47] methane dry reforming,[46,50,51] and toluene steam reforming.[47,52,53] In these investigations, they also developed kinetic models and studied the influence of synthesis parameters, such as metal precursor, metal loading, number of impregnations, and calcination temperature. Ni−olivine catalysts also reduced tars when added to fluidized-bed reactors during steam gasification of wood chips.[40,54] Zhang et al.[55] studied the promotional effect of adding CeO_2 to a Ni−olivine catalyst for reforming model tar compounds (benzene and toluene). They reported that CeO_2 addition led to improved tar destruction and greatly enhanced coke resistance.

(33) Anderson, J. R.; Foger, K.; Mole, T.; Rajadhyaksha, R. A.; Sanders, J. V. *J. Catal.* **1979**, *58*, 114.
(34) Perez-Ramirez, J.; Christensen, C. H.; Egeblad, K.; Christensen, C. H.; Groen, J. C. *Chem. Soc. Rev.* **2008**, *37*, 2530.
(35) Tao, Y.; Kanoh, H.; Abrams, L.; Kaneko, K. *Chem. Rev.* **2006**, *106*, 896.
(36) Wang, L.; Murata, K.; Inaba, M. *Appl. Catal., A* **2004**, *257*, 43.
(37) Xu, S.; Wang, X. *Fuel* **2005**, *84*, 563.
(38) Potdar, H.; Roh, H.; Jun, K.; Ji, M.; Liu, Z. *Catal. Lett.* **2002**, *84*, 95.
(39) Choudhary, V. R.; Mondal, K. C.; Mamman, A. S. *J. Catal.* **2005**, *233*, 36.
(40) Corella, J.; Toledo, J.; Padilla, R. *Energy Fuels* **2004**, *18*, 713.
(41) Kuhn, J. N.; Zhao, Z.; Felix, L. G.; Slimane, R. B.; Choi, C. W.; Ozkan, U. S. *Appl. Catal., B* **2008**, *81*, 14.
(42) Kuhn, J. N.; Zhao, Z.; Senefeld-Naber, A.; Felix, L. G.; Slimane, R. B.; Choi, C. W.; Ozkan, U. S. *Appl. Catal., A* **2008**, *341*, 43.
(43) Sutton, D.; Kelleher, B.; Ross, J. R. H. *Fuel Process. Technol.* **2001**, *73*, 155.
(44) El-Rub, Z.; Bramer, E.; Brem, G. *Ind. Eng. Chem. Res.* **2004**, *43*, 6911.
(45) Rapagna, S.; Jand, N.; Kiennemann, A.; Foscolo, P. U. *Biomass Bioenergy* **2000**, *19*, 187.
(46) Courson, C.; Makaga, E.; Petit, C.; Kiennemann, A. *Catal. Today* **2000**, *63*, 427.
(47) Swierczynski, D.; Courson, C.; Bedel, L.; Kiennemann, A.; Guille, J. *Chem. Mater.* **2006**, *18*, 4025.
(48) Devi, L.; Craje, M.; Thune, P.; Ptasinski, K. J.; Janssen, F. J. J. B. *Appl. Catal., A* **2005**, *294*, 68.
(49) Zhao, Z.; Kuhn, J. N.; Felix, L. G.; Slimane, R. B.; Choi, C. W.; Ozkan, U. S. *Ind. Eng. Chem. Res.* **2008**, *47*, 717.
(50) Courson, C.; Udron, L.; Swierczynski, D.; Petit, C.; Kiennemann, A. *Catal. Today* **2002**, *76*, 75.
(51) Courson, C.; Udron, L.; Swierczynski, D.; Petit, C.; Kiennemann, A. *Sci. Technol. Adv. Mater.* **2002**, *3*, 271.
(52) Swierczynski, D.; Libs, S.; Courson, C.; Kiennemann, A. *Appl. Catal., B* **2007**, *74*, 211.
(53) Swierczynski, D.; Courson, C.; Kiennemann, A. *Chem. Eng. Process.* **2008**, *47*, 508.
(54) Pfeifer, C.; Rauch, R.; Hofbauer, H. *Ind. Eng. Chem. Res.* **2004**, *43*, 1634.
(55) Zhang, R.; Wang, Y.; Brown, R. *Energy Convers. Manage.* **2007**, *48*, 68.

Characterization studies of Ni−olivine catalysts have shown several phases to be present, and multiple active sites have been proposed. Devi et al.[48,56] reported that calcination of olivine increased tar reforming activity and produced Fe^{3+} and other Fe species on the olivine surface, although the presence of metallic Fe formed in reducing conditions was thought necessary for efficient tar reforming to occur.[57] It has also been suggested that Mg contributes to tar destruction[42,48] and that calcination or reforming reactions on Ni−olivine led to the formation of Fe−Ni alloys[42,46,47,52,57] as well as solid solutions of NiO−MgO that are likely responsible for the high coke resistance of Ni/olivine catalysts.[47] Courson et al. showed that, when less Ni was added to olivine supports that naturally contained Fe, deactivation was more severe because of the formation of free iron oxide species that promoted the reverse water−gas shift reaction, which in turn, oxidized Ni to form inactive NiO.[51] Pfeifer et al.[54] tested Ni/olivine in a pilot-plant gasifier with wood pellets and 7.3 wt % steam and confirmed that the Ni/olivine catalyst had much higher tar conversion and was as attrition-resistant as unloaded olivine, showing no activity loss during 45 h of reaction testing. They also found that increasing the amount of catalyst led to a decrease in the produced syngas heating value.

Kuhn et al. studied olivine that was thermally impregnated with Ni for steam reforming using naphthalene, methane, ethylene, and methanol as the model compounds.[42,49] For these model compounds, they found higher conversions on Ni/olivine as compared to olivine. While Ni addition led to higher conversions for all of the tested compounds, some of the compounds were influenced to a greater extent than others. When Ni/olivine and olivine were compared, the conversion differences of model compounds were more pronounced when species were harder to activate (e.g., Ni addition affected methane more than naphthalene conversion, and methane is more stable than naphthalene). The authors also proposed that the basic nature of the olivine support and its propensity to form a hydroxylated surface during steam reforming leads to better ability for O−H bond scission as compared to C−H and C−C bonds. They experimentally showed that conversion of methanol during steam reforming was similar over olivine and Ni/olivine and speculated that this would hold for many oxygenated compounds.[42] They summarized the relative effect of Ni addition to olivine on conversion levels of model compounds as paraffins > olefins > aromatics > alcohols.[42]

Srinakruang et al.[58] compared the activity and coking resistance of Ni/dolomite to representative commercial catalysts (Ni/Al_2O_3 and Ni/SiO_2) during model tar reforming of a toluene/naphthalene mixture. They found that the support did not affect activity for nonsulfur-containing feed, but in the presence of H_2S, Ni/dolomite had superior resistance to coking and H_2S poisoning than either Ni/Al_2O_3 or Ni/SiO_2.

Asadullah et al.[59] compared dolomite, G-91 (a commercial Ni-based steam reforming catalyst), and $Rh/CeO_2/SiO_2$ for the gasification of ground cedar wood with ~10% water content. They found that the rhodium catalyst was more active and resistant to char and tar formation than any of the others materials that were tested.

Solid acid zeolites have been examined as supports for reforming catalysts and also as in-bed additives during gasification. Inaba et al.[60] studied Ni on CeO_2-promoted zeolites for biomass gasification. Acid sites found in zeolites promote both tar cracking and coking reactions, and although CeO_2 has been shown to reduce coking, coke formation was still observed on these catalysts. In addition to Ni, they also evaluated Rh supported on zeolites and found slightly higher activity on the Rh catalysts. Tests were carried out in a fluidized bed reactor, although attrition results were not reported.

For the gasification of commercially available cellulose, Tomishige et al.[61] found Rh to be a better catalyst than Ni-, Ru-, Pd-, and Pt-based catalysts on many different supports. Because these supports were not designed to withstand operation within a fluidized reactor, the authors observed appreciable attrition levels, although attrition was not quantified. The authors also tested Rh-catalyst-supported CeO_2/SiO_2, but these materials did not perform better than the Rh/CeO_2 and Rh/Al_2O_3 catalysts.

3.3. Reforming Catalyst Promoters. Promoting transition-metal-based catalysts with various elements can positively affect catalyst activity, reducibility, regenerability, and coke resistance. Promotion can also lead to improved mechanical strength and attrition resistance, which is important for catalysts used in fluidized-bed reactors. Studies on the effects of additives, such as Group VIII, transition, and alkali metals, are discussed below.

3.3.1. Group-VIII-Promoted Catalysts. The most commonly studied promoters for steam reforming, especially on Ni-based catalysts, are the Group VIII metals. Jeong et al.[62] looked at Ru doping of Ni supported on Al_2O_3 or $MgAl_2O_4$ for methane steam reforming. Ru addition led to decreased coke deposition, and the $MgAl_2O_4$-supported catalysts were more active than the Al_2O_3-supported catalysts. Li et al.[63] and Miyata et al.[64] also studied a material of similar composition, a Ru-promoted Ni/Mg(Al)O catalyst, for methane steam reforming. They observed that trace amounts of Ru stabilized the reforming activity and reducibility of Ni species, as indicated by TPR studies, and proposed that hydrogen spillover helped keep Ni in its active, reduced state.

Mukainakano et al.[65] studied the influence of the impregnation technique on Ni/Al_2O_3 catalysts promoted with precious metals (Pd and Rh) for SMR. They observed that catalysts prepared via sequential impregnation exhibited a more uniform temperature profile as compared to those prepared by co-impregnation. Additionally, it was found that Rh−Ni catalysts had higher CH_4 selectivity to CO than Pd−Ni catalysts.

Strohm et al.[66] studied the effect of the Rh/Ni ratio on the activity of $Rh/Ni/CeO_2-Al_2O_3$ catalysts for steam reforming a C_{13} hydrocarbon fuel (paraffinic NORPAR-13) with 100 ppm H_2S, simulating hydrocarbons from biomass gasification. They examined the effect of the Rh/Ni ratio on the reforming activity of $Rh/Ni/CeO_2-Al_2O_3$ catalysts and also concluded that the Rh/Ni bimetallic catalysts were superior to their monometallic counterparts for resistance to coking and sulfur poisoning.

The addition of cobalt to nickel catalysts has also been examined for syngas production from hydrocarbons and alco-

(56) Devi, L.; Ptasinski, K. J.; Janssen, F. J. J. B. *Fuel Process. Technol.* **2005**, *86*, 707.
(57) Swierczynski, D.; Courson, C.; Bedel, L.; Kiennemann, A.; Vilminot, S. *Chem. Mater.* **2006**, *18*, 897.
(58) Srinakruang, J.; Sato, K.; Vitidsant, T.; Fujimoto, K. *Fuel* **2006**, *85*, 2419.
(59) Asadullah, M.; Miyazawa, T.; Ito, S.; Kunimori, K.; Koyama, S.; Tomishige, K. *Biomass Bioenergy* **2004**, *26*, 269.
(60) Inaba, M.; Murata, K.; Saito, M.; Takahara, I. *Energy Fuels* **2006**, *20*, 432.
(61) Tomishige, K.; Asadullah, M.; Kunimori, K. *Catal. Surv. Asia* **2003**, *7*, 219.
(62) Jeong, J. H.; Lee, J. W.; Seo, D. J.; Seo, Y.; Yoon, W. L.; Lee, D. K.; Kim, D. H. *Appl. Catal., A* **2006**, *302*, 151.
(63) Li, D.; Atake, I.; Shishido, T.; Oumi, Y.; Sano, T.; Takehira, K. *J. Catal.* **2007**, *250*, 299.
(64) Miyata, T.; Shiraga, M.; Li, D.; Atake, I.; Shishido, T.; Oumi, Y.; Sano, T.; Takehira, K. *Catal. Commun.* **2007**, *8*, 447.
(65) Mukainakano, Y.; Li, B.; Kado, S.; Miyazawa, T.; Okumura, K.; Miyao, T.; Naito, S.; Kunimori, K.; Tomishige, K. *Appl. Catal., A* **2007**, *318*, 252.
(66) Strohm, J.; Zheng, J.; Song, C. *J. Catal.* **2006**, *238*, 309.

hols. Homs et al.[67] examined a Co−Ni/ZnO catalyst for ethanol steam reforming at 500 °C. Reaction experiments and XPS analysis indicated that co-addition led to improved coking resistance on the Co−Ni catalyst. Moon and Ryu[68] doped Ni-based catalysts with Co and Fe for the partial oxidation of isooctane in the presence of H_2S. In comparison to unpromoted, commercial Ni-based reforming catalysts, the doped materials showed higher activity and stability. These materials also resisted the formation of metal carbides, because neither Ni nor Fe carbide was observed by postreaction XRD after 750 h time-on-stream.

3.3.2. Transition-Metal-Promoted Catalysts. Transition metals are another class of promoters that have been incorporated into Ni-based catalysts and studied for their effects on reforming reactions. Chin et al.[69] used Au−Ni bimetallic catalysts for SMR. They observed higher methane conversion on the monometallic Ni catalyst than on the Au−Ni bimetallic catalyst. After butane steam reforming, thermogravimetric analysis (TGA) studies of the Au−Ni catalysts showed lower coke deposition below 500 °C but higher coke deposition at 550 °C as compared to the Ni-only catalyst. Work from the Bueno group[70,71] examined Ag−Ni catalysts used for methane and ethanol steam reforming. They found that the addition of Ag to Ni/Al_2O_3 led to lower reforming activity but increased resistance to deactivation by coking because of the suppression of bridged carbonyl species, decreased adsorbed carbon formation rate, and geometric effects of Ag blocking Ni sites for nucleation of graphite. Increasing Ag loading also led to an increase in the apparent activation energy for methane reforming. Youn et al.[72] studied ethanol ATR on Ni/Al_2O_3 with various promoters (Cu, Co, Zn, Ce, and Mg). The highest activity, achieved with the Cu-promoted sample, was attributed to increased Ni reducibility and negligible Ni sintering.

Garcia et al.[73] looked at bio-oil reforming using two promotion strategies to improve coke resistance of $Ni/\alpha\text{-}Al_2O_3$ catalysts. The first strategy used Mg and La to increase steam adsorption to enhance gasification of surface-deposited carbon. The second strategy added Co and Cr to slow the rate of the coke formation reaction on the surface. The promoters led to improved stability of the catalysts as compared to conventional, unpromoted Ni/Al_2O_3 materials and also appeared to promote the water−gas shift reaction.

3.3.3. Alkali-Promoted Catalysts. The promotion by alkali metals, especially potassium, is another strategy used to improve reforming catalysts. Promotion by alkali metals has been found to increase stability, possibly by enhanced spillover of adsorbed steam.[74] Juan et al.[75] varied potassium loading on Ni/Al_2O_3 catalysts used for methane steam reforming and discovered that K addition led to reduced coking and also reduced catalytic activity. These K-promoted catalysts showed good stability for methane steam reforming for 24 h. Snoeck et al.[76] developed a kinetic model to describe the rates of carbon formation and gasification on potassium-promoted nickel catalysts. The authors found that increasing potassium content led to decreased carbon formation, while an optimal potassium loading provided a maximum rate of gasification, above which more potassium addition led to a decrease in the reaction rate. Qi et al.[77] studied Ni/Al_2O_3 catalysts promoted with K and Na for methanol steam reforming at 400 °C and found that the Ni/Al_2O_3 catalysts promoted with K had a higher H_2 production rate than those promoted with Na. Frusteri et al.[78] examined Ni/MgO catalysts promoted with Na, Li, or K for ethanol steam reforming at 650 °C. They found that alkali promotion led to higher ethanol conversion and selectivity to methane. The promotion with Na and Li led to enhanced NiO reducibility but decreased dispersion of the Ni/MgO catalysts.

3.3.4. Other Promoted Catalysts. Zhang et al.[55] studied the effect of CeO_2 addition to a Ni/olivine catalyst for steam reforming of benzene or toluene. CeO_2 is well-known to undergo redox cycles and for its ability to donate oxygen, and the authors found that its addition to Ni/olivine enhanced tar conversion, H_2 production, and coke resistance. Benito et al.[79] examined the effect of La_2O_3 addition to Ni/Al_2O_3 for CH_4/CO_2 reforming at 700 °C. They observed that La_2O_3 promotion led to increased stability, likely because of oxygen donation from $La_2O_2CO_3$ species to produce CO from carbon deposits.

Xu and Saeys[80] used density functional theory (DFT) calculations to predict the anti-coking effect of adding boron to Ni-based catalysts. Their calculations show that chemisorbed carbon species diffuse into the octahedral sites of the Ni catalyst and that boron atoms also preferentially adsorb to octahedral sites on the first subsurface layer. On the basis of these results, they propose boron as a good anti-coking promoter for nickel catalysts. Nikolla et al.[81,82] used a hybrid theoretical/experimental approach to predict and experimentally show improved coke resistance to Sn-promoted nickel catalysts for methane and isooctane steam reforming, and these studies are further discussed in Section 4.1.1. Coke-Resistant Catalytic Studies.

Trimetallic $LaNi_{0.3}Fe_{0.7}O_3$ perovskite catalysts were examined by Rapagna et al.[83] for SMR and conditioning biomass gasification vapors. These materials showed both high methane conversion and resistance to carbonaceous deposits. Ceria and perovskite materials have high oxygen mobility, creating pools of oxygen that can be used to gasify surface carbon and promote coking resistance. Materials such as transition-metal carbides have also been studied for steam reforming.[84] These materials have the advantage of being relatively abundant and cheap and are often prepared using metal oxide precursors. Molybdenum carbide has been shown to be active and stable for hydrocarbon reforming and resistant to coking.[85,86] Carbides, however, only

(67) Homs, N.; Llorca, J.; Ramirez de la Piscina, P. *Catal. Today* **2006**, *116*, 361.
(68) Moon, D.; Ryu, J. *Catal. Lett.* **2003**, *89*, 207.
(69) Chin, Y.; King, D.; Roh, H.; Wang, Y.; Heald, S. *J. Catal.* **2006**, *244*, 153.
(70) Parizotto, N. V.; Rocha, K. O.; Damyanova, S.; Passos, F. B.; Zanchet, D.; Marques, C. M. P.; Bueno, J. M. C. *Appl. Catal., A* **2007**, *330*, 12.
(71) Liberatori, J.; Ribeiro, R.; Zanchet, D.; Noronha, F.; Bueno, J. *Appl. Catal., A* **2007**, *327*, 197.
(72) Youn, M.; Seo, J.; Kim, P.; Kim, J.; Lee, H.; Song, I. *J. Power Sources* **2006**, *162*, 1270.
(73) Garcia, L.; French, R.; Czernik, S.; Chornet, E. *Appl. Catal., A* **2000**, *201*, 225.
(74) Rostrup-Nielsen, J. R.; Sehested, J. *Adv. Catal.* **2002**, *47*, 65.
(75) Juan, J.; Roman-Martinez, M.; Illan-Gomez, M. *Appl. Catal., A* **2006**, *301*, 9.
(76) Snoeck, J. W.; Froment, G. F.; Fowles, M. *Ind. Eng. Chem. Res.* **2002**, *41*, 3548.
(77) Qi, C.; Amphlett, J.; Peppley, B. *J. Power Sources* **2007**, *171*, 842.
(78) Frusteri, F.; Freni, S.; Chiodo, V.; Spadaro, L.; Di Blasi, O.; Bonura, G.; Cavallaro, S. *Appl. Catal., A* **2004**, *270*, 1.
(79) Benito, M.; Garcia, S.; Ferreira-Aparicio, P.; Garcia Serrano, L.; Daza, L. *J. Power Sources* **2007**, *169*, 177.
(80) Xu, J.; Saeys, M. *J. Catal.* **2006**, *242*, 217.
(81) Nikolla, E.; Holewinski, A.; Schwank, J.; Linic, S. *J. Am. Chem. Soc.* **2006**, *128*, 11354.
(82) Nikolla, E.; Schwank, J.; Linic, S. *J. Catal.* **2007**, *250*, 85.
(83) Rapagna, S.; Provendier, H.; Petit, C.; Kiennemann, A.; Foscolo, P. U. *Biomass Bioenergy* **2002**, *22*, 377.
(84) Christofoletti, T.; Assaf, J. M.; Assaf, E. M. *Chem. Eng. J. (Amsterdam, Neth.)* **2005**, *106*, 97.
(85) Ross, J. R. H. *Catal. Today* **2005**, *100*, 151.
(86) Lee, J. S.; Oyama, S. T.; Boudart, M. *J. Catal.* **1987**, *106*, 125.

Table 4. General Catalyst Deactivation Processes

type	cause	result
mechanical	particle failure	bed channeling, plugging
	fouling	loss of surface
thermal	component volatilization	loss of component
	phase changes	loss of surface
	compound formation	loss of component and surface
	sintering	loss of surface
chemical	poison adsorption	loss of active sites
	coking	loss of surface, plugging

maintain their activity for dry reforming in conditions where the carbide is stable in the presence of a CO_2 reaction mixture.[85]

4. Catalyst Deactivation

The activity and lifetime of a catalyst are two essential components governing the economic feasibility of using a catalytic conditioning process. While all catalysts will lose initial performance, the activity loss in a well-controlled process should be slow.[87] The undesirable deactivation of catalysts during their extended use can occur through several routes. Spencer and Twigg[88] completed an extensive study on catalyst deactivation and found three general deactivation modes that apply to most catalytic systems: (1) mechanical, (2) thermal, and (3) chemical. These modes are distinguishable by various changes that alter the available surface area and chemical and physical nature of the active sites, leading to an observed change in the overall rate of reaction. Examples of these deactivation modes are listed in Table 4.

Mechanical and thermal deactivation processes can be significant because of the high temperatures and harsh reaction conditions, which may be present during conditioning of biomass-derived syngas. Although optimization of the reactor system and process conditions can help reduce the influence of these deactivation mechanisms, resistance to attrition, sintering, phase changes, and volatilization must all be considered during the development of an industrially viable catalytic material. While mechanical and thermal deactivation processes are of concern, resistance to chemical deactivation plays an even more vital role in the development of catalysts for raw biomass-derived syngas conditioning.

The catalysts currently used for raw syngas conditioning are susceptible to time-on-stream deactivation, primarily through coking and sulfidation (sulfur poisoning).[8] These deactivation processes are significant process obstacles that must be overcome. The fundamental understanding of these processes as they relate to base catalysts and specific syngas compositions will be helpful in designing catalysts to minimize the degradation of long-term catalytic performance.

The first of these routes, coking, occurs when hydrocarbons first activate on a catalytic surface and then subsequently dissociate. This dissociation leads to surface carbon that can nucleate to form larger carbon deposits and graphitic sheets, which then cover the catalyst surface and block active sites. Evidence from transmission electron microscopy (TEM) shows that carbon deposits are responsible for undermining metallic nickel species, which can then flake off the catalyst surface. Carbidic carbon formation is also possible. The second major deactivation mechanism, sulfidation, comes from catalyst interaction with sulfur-containing species, which may be present in the range of 50−500 ppm of sulfur (mainly as H_2S) in biomass-derived syngas. Once sulfur compounds have been activated on the catalyst surface, the adsorbed sulfur species

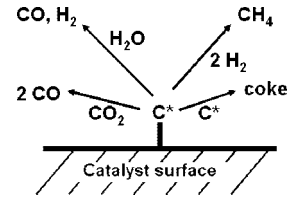

Figure 2. Reaction pathways of adsorbed carbon.

can bind to the active metal surface to form an inactive metal sulfide.[7,74] Coking and sulfidation are not unique to syngas-conditioning catalysts, because these deactivation modes are also significant problems in the petrochemical and coal industries, and have been researched for decades.

4.1. Coke Formation. Carbonaceous deposits (coke) on a catalyst can cover the surface and prevent reactants from reaching active metal sites.[89] These carbon deposits can occur in many different forms, including amorphous films or fibers, adsorbed carbides, and crystalline graphitic sheets. Some of these forms of carbon remain on the surface, while others diffuse into the catalyst. Because of the chemical and physical variations of coking, different forms of coke can require different removal methods.[87,90]

The breadth of coking chemistry as applied to steam reforming hydrocarbons and syngas conditioning has been reviewed by Rostrup-Nielsen.[74,91] The type of hydrocarbons interacting with a catalyst affects the amount of coke that is formed, and the general propensity for coke formation of hydrocarbon species is aromatic > olefinic > paraffinic. On metals, one route to coking deactivation is the formation of carbon "whiskers" that grow without intrinsically deactivating the metal site but can cause the metallic catalyst sites to breakdown via physical flaking off from the support surface. At high temperatures, another significant process is the encapsulation of catalyst particles with pyrolytic coke formed from small hydrocarbons, such as ethylene, contained in the raw syngas and produced from pyrolysis of higher hydrocarbons present during tar cracking.

A macroscopic view of possible reaction pathways for adsorbed carbon (C*) is shown in Figure 2. The first process is the activation of hydrocarbons (or other carbonaceous species) to form carbon deposits. These carbon deposits then have several reaction pathways that they can follow. Carbon deposits can react with activated steam or CO_2 to form C−O bonds and produce CO. They can also react with H_2 to form CH_4. An alternative, undesired pathway is carbon nucleation, the reaction of C* with another C* to form C−C bonds and create coke deposits. While this schematic excludes some specific steps of proposed coking mechanisms, such as carbon dissolution into the metal and diffusion across the particle (which can be found elsewhere),[92] it provides a general view of how coking occurs and might be controlled.

Considering the reaction network shown in Figure 2, the overall level or rate of coke formation may be adjusted by changing the relative rates of reaction for (1) carbon deposition, (2) carbon nucleation or C−C bond formation on the catalyst surface, or (3) C−O bond formation. For example, an increased oxidant (steam and oxygen) concentration leads to an increased gasification rate and a lower coking rate. Although changes in

(87) Bartholomew, C. *Appl. Catal., A* **2001**, *212*, 17.
(88) Spencer, M.; Twigg, M. *Annu. Rev. Mater. Res.* **2005**, *35*, 427.
(89) Aguayo, A.; Gayubo, A.; Erena, J.; Atutxa, A.; Bilbao, J. *Ind. Eng. Chem. Res.* **2003**, *42*, 3914.
(90) Ginsburg, J.; Pina, J.; Solh, T.; Lasa, H. *Ind. Eng. Chem. Res.* **2005**, *44*, 4846.
(91) Rostrup-Nielsen, J. *Catal. Today* **1997**, *37*, 225.
(92) Trimm, D. L. *Catal. Today* **1997**, *37*, 233.

the concentrations of the gaseous species, such as hydrocarbons or steam, can be achieved through various process strategies, which then affect the overall rates of adsorption, desorption, and surface reactions because of changes in surface coverage from Le Chatelier's principle, this discussion will be restricted to catalyst changes that have been shown to significantly affect overall coking rates.

4.1.1. Coke-Resistant Catalytic Studies. The rate of carbon nucleation (i.e., coking) has been investigated along with attempts to slow this process. Theoretical density functional theory (DFT) models have shown that nickel particle size affects the rate of carbon nucleation and particles smaller than a critical size around 25 Å do not provide an energetically favorable environment for carbon nucleation to form graphitic sheets.[74] Experimental evidence confirmed this prediction by showing that small nickel particles (<50 Å) did not exhibit graphite formation, and the onset of carbon deposition on small Ni crystallites (7 nm) occurred at 100 °C lower temperature than on larger Ni crystallites (100 nm).[74,93] In addition to controlling metallic particle size, coking on catalysts has also been controlled through the use of promoters/additives. On nickel surfaces, promoters, such as potassium, gold, and sulfur,[93,94] preferentially bind to step edge sites. Nickel step edge sites are thought to be highly active for carbon nucleation; therefore, blocking these sites by promoting (protecting) Ni with these elements leads to decreased rates of carbon nucleation and coking.[74,95] This idea is connected to the strategies behind catalyst promotion, which can lead to changes in the relative rates of desired and undesired reactions.

The site-specific adsorption caused by promoters can work by either blocking the active site for a deactivation mechanism (e.g., coking) or altering the kinetic properties of neighboring sites, which is sometimes referred to as an *ensemble effect*. The ensemble effect may occur if the reaction intermediate for gasification involves fewer surface atoms than the one for coke formation.[74] When an adsorption site is active for both desired and undesired reactions (e.g., reforming and coking), the activity changes following promotion will depend upon the activities of the remaining active sites for each reaction. Once the most active sites (primary) for both the desired and undesired reactions are blocked, the next-most active sites (secondary) dictate reaction rates.

Nikolla et al.[81,82] used DFT calculations to predict anti-coking behavior of tin-promoted nickel, which they also verified experimentally for the reforming of methane, propane, and isooctane. They postulated that a coke-resistant catalyst must be able to efficiently oxidize adsorbed carbon and prevent formation of C−C bonds. Their DFT model showed that, on a pure Ni surface, similar energy barriers for C diffusion to form C−C bonds and O diffusion to form C−O bonds were observed. The addition of tin, however, led to an increase in the energy barrier for the diffusion to form both C−C and C−O bonds. Although both the rate of carbon removal and coke formation were slowed, the energy barrier was raised to a greater extent for the C−C bond formation as opposed to the C−O bond formation. Therefore, the relative rate of carbon removal as compared to coke formation was increased, which led to the observed anti-coking behavior.

Increasing the reaction pathway for carbon oxidation can also decrease coking. Chang et al. compared Ni/ZrO_2 to $Ni/Ce\text{-}ZrO_2$ for dry methane reforming and explained that the presence of CeO_2 led to improved stability by increasing the concentration of highly mobile oxygen species, which helped prevent coking.[96] They proposed a stable, solid solution between ZrO_2 and CeO_2 with a high capacity for oxygen storage and affinity for CO_2. In reducing conditions, partially reduced CeO_2 promoted CO_2 dissociation to provide activated oxygen species. Zhang et al. examined various metals (Co, Ir, and Ni) supported on CeO_2 for steam reforming bioethanol.[20] While these materials showed activity loss with extended time-on-stream, because of metal sintering and some coking, the high oxygen-storage release capacity of ceria continued to facilitate coke gasification.

The use of alternate base metals, such as Ru and Rh (as opposed to Ni) in steam reforming has also been shown to retard coke formation. This is attributed to the greater ability of carbon to dissolve in Ni than Ru or Rh, which can be thought of as a higher rate of carbon deposition/dissolution on Ni surfaces.[92] The metal substitution or promotion of Ni catalysts with Ru or Rh can therefore lead to a decrease in the rate of carbon deposition and coking.

Through understanding adsorption site activity and diffusion energetics, as well as the mechanisms underlying coke formation, researchers have made significant contributions in designing coke-resistant catalysts. These insights will be valuable for adapting the previous art to address deactivation via coking during the catalytic conditioning of biomass-derived syngas.

4.2. Sulfur Poisoning. Poisoning or deactivation may occur on a catalyst surface by either nonselective adsorption of the poison on many sites or by selective adsorption onto only specific active sites. Sulfur is known to selectively adsorb and form metal sulfides on many materials. Dependent upon the deactivating species, the adsorption may be reversible or irreversible. The deactivation of Ni catalysts through sulfur poisoning has been studied by many investigators[88,97−101] and has been described by the formation of nickel sulfide, as shown in eq 5. Work at NREL on a Ni/Al_2O_3-type catalysts exposed to H_2S[101] and other authors propose that a nickel sulfide (or, in general, a metal sulfide) can be regenerated with steam treatment to form H_2S and a metal oxide, followed by reduction in H_2 to recover the reduced metal as shown in eqs 6 and 7[102,103]

$$Ni + H_2S \leftrightarrow Ni{-}S + H_2 \quad (5)$$

$$Ni{-}S + H_2O \leftrightarrow NiO + H_2S \quad (6)$$

$$NiO + H_2 \leftrightarrow Ni + H_2O \quad (7)$$

Much work has focused on the problem of catalyst sulfur poisoning, and representative studies of development of sulfur-tolerant materials are discussed. One approach to mitigating the

(93) Bengaard, H. S.; Norskov, J. K.; Sehested, J.; Clausen, B. S.; Nielsen, L. P.; Molenbroek, A. M.; Rostrup-Nielsen, J. R. *J. Catal.* **2002**, *209*, 365.
(94) Besenbacher, F.; Chorkendorff, I.; Clausen, B. S.; Hammer, B.; Molenbroek, A. M.; Norskov, J. K.; Stensgaard, I. *Science* **1998**, *279*, 1913.
(95) Abild-Pedersen, F.; Lytken, O.; Engbaek, J.; Nielsen, G.; Chorkendorff, I.; Norskov, J. K. *Surf. Sci.* **2005**, *590*, 127.
(96) Chang, J.-S.; Hong, D.-Y.; Li, X.; Park, S.-E. *Catal. Today* **2006**, *115*, 186.
(97) Ko, T.; Chu, H.; Chaung, L. *Chemosphere* **2005**, *58*, 467.
(98) Cheekatamarla, P.; Lane, A. *J. Power Sources* **2006**, *154*, 223.
(99) Koizumi, N.; Murai, K.; Ozaki, T.; Yamada, M. *Catal. Today* **2004**, *89*, 465.
(100) Wang, Z.; Flytzani-Stephanopoulos, M. *Energy Fuels* **2005**, *19*, 2089.
(101) Magrini-Bair, K. A.; Czernik, S.; French, R.; Parent, Y. O.; Chornet, E.; Dayton, D. C.; Feik, C.; Bain, R. *Appl. Catal., A* **2007**, *318*, 199.
(102) Lombard, C.; Le Doze, S.; Marencak, E.; Marquaire, P.-M.; Le Noc, D.; Bertrand, G.; Lapicque, F. *Int. J. Hydrogen Energy* **2006**, *31*, 437.
(103) Bartholomew, C. H.; Agrawal, P. K.; Katzer, J. R. *Adv. Catal.* **1982**, *31*, 173.

adverse effects of H_2S in gasified biomass streams is to develop more sulfur-tolerant catalysts. Another approach is the upstream removal of H_2S from the gas stream. A common approach in the coal industry is the use of a sulfur sorbent, such as ZnO, to adsorb H_2S, forming ZnS, to protect water−gas shift catalysts from poisoning. The catalytic conditioning of biomass-derived syngas streams, however, currently occurs at temperatures that are too high (~800 °C) for ZnO sorbents, which have an upper limit for efficient H_2S adsorption of 500 °C.[104,105] Nonetheless, this same approach may be used for biomass tar conditioning if a suitable sulfur sorbent can be developed that tolerates the process conditions of high temperature and high steam content.

4.2.1. Sulfur-Resistant Catalytic Studies. The development of catalysts that are resistant to coking and sulfur poisoning (mainly H_2S) is often performed simultaneously. It should be noted that, while sulfur is well-known to deactivate metals and Ni, in particular, sulfidation can also lead to reduced coke formation through the ensemble effect, whereby sites neighboring a poisoned site are physically blocked or electronically altered.[106] As noted in Section 4.1.1. Coke-Resistant Catalytic Studies, sulfur preferentially binds to partially uncoordinated step edge sites that are active for carbon nucleation and blockage of these sites, whether by a material considered a promoter or a poison, such as sulfur, results in decreased coking rates.[93,94]

Sato and Fujimoto[107] examined tar reforming of naphthalene on a Ni/MgO−CaO catalyst promoted with WO_3 for sulfur resistance. Studies showed that increased WO_3 loading led to improved resistance to H_2S deactivation. The proposed mechanism involved the reaction of W with Ni−S to form W−S, which can then react with H_2 to form and desorb H_2S from the catalyst surface. These authors also studied Ni/dolomite for naphthalene and toluene reforming and found that, in the presence of H_2, deactivation of Ni/dolomite by sulfur poisoning was reversible, because the initial reforming activity could be regained when H_2S was removed from the feed stream.[58]

Srinakruang et al. synthesized Ni/dolomite catalysts, which they reported to be more sulfur- and coke-resistant than Ni/Al_2O_3 and Ni/SiO_2 catalysts in the presence of 100 ppm H_2S for toluene and naphthalene steam reforming.[58] They also observed that the poisoning effect on Ni/dolomite was reversible and activity was regained when H_2S was removed from the stream. Additionally, when the temperature was increased from 770 to 850 °C, the detrimental effect of H_2S decreased.

Tomishige et al. gasified cedar wood chips in a fluidized bed reactor and determined product gas compositions obtained with a commercial Ni steam reforming catalyst and a Rh/CeO_2/SiO_2 catalyst with and without H_2S.[108] Both catalysts showed a decrease in the rate of CO and H_2 formation upon the addition of H_2S, although the Rh/CeO_2/SiO_2 catalyst was more stable than the Ni catalyst, which was severely deactivated. Although single crystal studies show that sulfur should strongly adsorb on both Ni and Rh, each catalyst deactivated differently. The authors propose the importance of a redox cycle of the active metal within the fluidized bed reactor, as it moves between reducing and oxidizing environments. On the Ni catalyst, sulfur was adsorbed on the catalyst as SO_4^{2-} and Ni was oxidized to NiO. The addition of H_2S prevented the reduction of NiO to Ni, causing the loss of reforming activity. Although the mechanism is not fully understood, on the Rh/CeO_2/SiO_2 catalyst, H_2S is reversibly adsorbed and the CeO_2 component is proposed to promote the removal of sulfur adsorbed on Rh as H_2S, COS, and SO_2.

Bain et al.[8] used a slipstream of gasified wood from a pilot plant to conduct studies modeling the deactivation kinetics of Ni/Mg/K/Al_2O_3 catalysts used for syngas conditioning in a fluidized-bed reactor. The deactivation was modeled using first- and second-order kinetic models, and activation energies for the destruction of the individual compounds (e.g., methane, ethane, benzene, and tars) found in the syngas were reported. While both first- and second-order deactivation models fit the data relatively well, a comparison of the activation energies indicated that first-order kinetics provided a more realistic estimate for the catalyst deactivation during raw syngas conditioning.

Cheekatamarla and Lane studied sulfur-tolerant, bimetallic catalysts for the autothermal reforming of synthetic diesel and JP8 fuel.[109] They examined bimetallic Pt−Ni/CeO_2 and Pt−Pd/Al_2O_3, as well as the monometallic catalysts on the respective supports. They found that the bimetallic catalysts had higher ATR activity and improved resistance to sulfur poisoning than the monometallic counterparts. The improved performance was attributed to structural and electronic effects, resulting in strong metal−metal and strong metal−support interactions.

4.3. Effects of Trace Contaminants. In addition to sulfur poisoning, poisoning by other contaminants that are naturally present in biomass may also contribute to catalyst deactivation. Elemental analysis of biomass feedstocks by the National Renewable Energy Laboratory (NREL) and the Pacific Northwest National Laboratory (PNNL) showed the presence of many inorganic species, namely, Si, Al, Ti, Fe, Ca, Mg, Na, K, P, S, and Cl.[8,110] Elliott et al. looked at the effects of these contaminants on a Ru/TiO_2 catalyst for aqueous-phase hydrogenation of sugars.[110] This study showed that these trace contaminants negatively affected catalyst activity, which was attributed to a combination of competitive adsorption and poisoning. While this system has many differences as compared to the gaseous tar reforming system, the study offers some insight into the effects of catalyst exposure to the trace contaminants found in biomass.

Trembly et al. studied the effects of trace coal contaminants on solid oxide fuel cell (SOFC) performance in coal-derived syngas.[111,112] Coal, which originates from organic biomass materials, contains the same inorganic impurities that are found in biomass, as well as many other inorganic impurities.[111] Additionally, the Ni catalysts used in SOFCs are similar to Ni tar reforming catalysts. While the negative effects of sulfur and chlorine on SOFC catalyst performance are recognized, studies on the other trace contaminants are needed.[111] Trace contaminants can be classified on the basis of their volatility and partitioning between gaseous and condensed phases[111] (e.g., char), which dictates which impurities would interact with a tar reforming catalyst. The cumulative effects of low levels of trace contaminants contained in biomass, however, represent an area of research that requires additional studies on realistic

(104) Jung, S. Y.; Lee, S. J.; Lee, T. J.; Ryu, C. K.; Kim, J. C. *Catal. Today* **2006**, *111*, 217.
(105) Slimane, R.; Williams, B. *Ind. Eng. Chem. Res.* **2002**, *41*, 5676.
(106) Erekson, E. J.; Bartholomew, C. H. *Appl. Catal., A* **1983**, *5*, 323.
(107) Sato, K.; Fujimoto, K. *Catal. Commun.* **2007**, *8*, 1697.
(108) Tomishige, K.; Miyazawa, T.; Kimura, T.; Kunimori, K.; Koizumi, N.; Yamada, M. *Appl. Catal., B* **2005**, *60*, 299.
(109) Cheekatamarla, P. K.; Lane, A. M. *J. Power Sources* **2006**, *153*, 157.
(110) Elliott, D. C.; Peterson, K. L.; Muzatko, D. S.; Alderson, E. V.; Hart, T. R.; Neuenschwander, G. G. *Appl. Biochem. Biotechnol.* **2004**, *115*, 807.
(111) Trembly, J. P.; Gemmen, R. S.; Bayless, D. J. *J. Power Sources* **2007**, *163*, 986.
(112) Trembly, J. P.; Gemmen, R. S.; Bayless, D. J. *J. Power Sources* **2007**, *169*, 347.

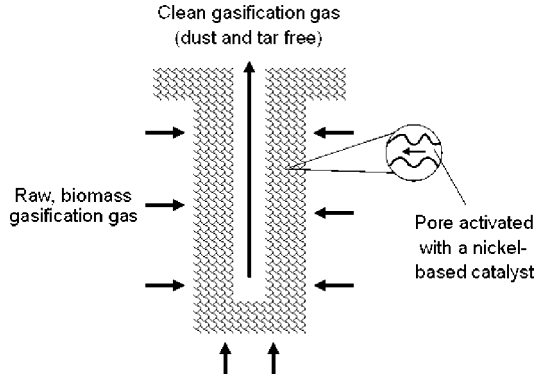

Figure 3. Schematic of a candle filter.

systems before suitable biomass-derived syngas conditioning catalysts can be deployed on a commercial scale.

5. Catalytic Filters and Monolith Reactors

Most commercially available Ni-based catalysts for steam reforming are designed for fixed-bed use and are often made to have a pellet, ring, or spherical shapes.[113] It has been verified that coating ceramic elements, such as candle filters and monoliths, with catalyst layers can lead to increased conversion of the reformate. This section discusses studies of catalytic filters and monoliths related to reforming of biomass-derived compounds, and a discussion of the history and industrial applications of monolithic reactors can be found in a review by Dudukovic et al.[114]

Candle filters have been studied extensively by a group at Vrije Universiteit Brussel. The basic structure of the candle filter as depicted by Engelen et al.[115] is shown in Figure 3. The filter contains a cracking catalyst preferentially deposited in the filter pores and thus does not have the internal mass transfer limitations that pellet catalysts have. The group demonstrated complete conversion of toluene and benzene in 100 ppm H_2S at 900 °C using their candle filters.[116,117] Catalyst compositions of the candle filter studies performed by the Vrije Universiteit Brussel group are given in Table 5.

Catalytic monoliths have been studied extensively by Corella et al.,[113,118−120] who published a four-part series comprising (1) tar reforming efficiency and deactivation, (2) modeling, (3) efficiency of NH_3 elimination, and (4) next-generation monolith designs. In part 1, monoliths are compared to commercial steam reforming Ni catalysts and dolomites with the overall conclusion that the monoliths have similar activity and deactivate almost as quickly as the commercial catalysts and dolomite. Because the monolith is significantly more expensive to produce than the commercial catalysts and dolomite, it is currently a less economic choice for tar removal from syngas, although advances in fabrication could reduce cost. The second part of the study applies a macrokinetic, one-dimensional model to the monolithic reactor to determine effective rate constants for NH_3 and tar elimination reactions, which were used to compare the activity between monolith reactors to commercial powdered/shaped catalysts and dolomite. Part 3 of the Corella series discusses NH_3 conversion in a nickel-coated monolithic catalyst located downstream of a gasification unit using pine wood chips as feed stock. Resultant poor ammonia conversion was attributed to poor heat integration in the monolith, with significant losses occurring through the reactor walls. Because tar cracking is an endothermic reaction and thus strongly dependent upon temperature, heat loss meant that the reaction slowed down the length of the monolith. Plugging was also a problem because the product gas stream contained particulates. In the fourth part of the study, integration of the gasifier and monolithic reactor was optimized with the addition of a two-layer monolith containing an interlayer heater to minimize thermal losses. Subsequent tests showed that the two-layer monolith had higher conversion and more coke resistance than the single-layer monolith tested in earlier studies. The results from the Corella work identified three key parameters for operating a feasible monolithic catalytic conditioning system: (1) total air flow partitioning, (2) a low alkali content of the feedstock to prevent monolith coating and plugging by ash, and (3) alternate catalyst compositions that yield high tar conversion at lower temperatures.

Suetsana et al.[121] synthesized a Cu−Ni rectangular monolith reactor and found the activity for both dry CH_4/CO reforming and methanol reforming to be greater than 99%. For methanol steam reforming at 400 °C, the honeycomb monoliths were more selective toward H_2 but produced 20% more CO_2 than dry methane reforming at 800 °C. Both the CO_2 yield and H_2 selectivity were reduced when the space velocity was lowered from 2600 to 1600 h^{-1}. Monolith activity to condition pine-derived syngas was low, although its ability to operate in the presence of particulates was a benefit.[113,118−120] Further work with actual syngas, monolith design, and catalytic coatings will determine how well these kinds of reactors can perform.

6. Fixed- versus Fluidized-Bed Operation

Most studies of steam reforming catalysts have been performed in fixed-bed reactor systems, although recent work has compared fixed- and fluidized-bed reactors for both steam and dry methane reforming performance with Ni-based catalysts, which are listed in Table 6.

Effendi et al. studied Ni/Al_2O_3[122] and Ni/SiO_2[123] in both fixed- and fluidized-bed reactors for steam and dry reforming of methane, respectively. With both catalysts, the fluidized-bed reactor showed higher CH_4 conversion and lower coke formation as compared to the fixed bed. Chen et al.[124] reported a similar result with a Ni/Al_2O_3 catalyst used for the dry reforming of methane at 800 °C. Under fluidized bed operation, conversion increased and coking decreased. Neither study reported attrition, although Effendi noted that attrition was a problem for fluidized-bed operation.

Attrition is a major factor that limits the types of materials that can be used in a fluidized-bed reactor. High-strength materials, such as olivine and specially designed catalysts, are suitable for use in a fluidized environment, whereas materials

(113) Corella, J.; Toledo, J.; Padilla, R. *Ind. Eng. Chem. Res.* **2004**, *43*, 2433.
(114) Dudukovic, M. P.; Larachi, F.; Mills, P. L. *Cat. Rev.* **2002**, *44*, 123.
(115) Engelen, K.; Zhang, Y.; Draelants, D.; Baron, G. *Chem. Eng. Sci.* **2003**, *58*, 665.
(116) Ma, L.; Verelst, H.; Baron, G. *Catal. Today* **2005**, *105*, 729.
(117) Nacken, M.; Ma, L.; Engelen, K.; Heidenreich, S.; Baron, G. *Ind. Eng. Chem. Res.* **2007**, *46*, 1945.
(118) Corella, J.; Toledo, J.; Padilla, R. *Ind. Eng. Chem. Res.* **2006**, *45*, 1389.
(119) Corella, J.; Toledo, J.; Padilla, R. *Ind. Eng. Chem. Res.* **2005**, *44*, 2036.
(120) Corella, J.; Toledo, J.; Padilla, R. *Ind. Eng. Chem. Res.* **2004**, *43*, 8207.
(121) Suetsuna, T.; Suenaga, S.; Fukasawa, T. *Appl. Catal., A* **2004**, *276*, 275.
(122) Effendi, A.; Zhang, Z.; Hellgardt, K.; Honda, K.; Yoshida, T. *Catal. Today* **2002**, *77*, 181.
(123) Effendi, A.; Hellgardt, K.; Zhang, Z.; Yoshida, T. *Catal. Commun.* **2003**, *4*, 203.
(124) Chen, X.; Honda, K.; Zhang, Z. *Catal. Today* **2004**, *93−95*, 87.

Table 5. Catalytic Candle Filter Studies for Conditioning Reactions

metal	promoter	support	reaction	conditions	references
Ni	MgO	Al_2O_3	model syngas, C_6H_6, $C_{10}H_8$	900 °C	116
Ni	Ca	Al_2O_3	model syngas, C_6H_6, $C_{10}H_8$	700−900 °C	117
Ni	Ru, Ca	Al_2O_3	model syngas, C_6H_6, $C_{10}H_8$	700−900 °C	117
Ni		dolomite	model syngas, C_6H_6, $C_{10}H_8$	700−900 °C	117
Ni	Ru	dolomite	model syngas, C_6H_6, $C_{10}H_8$	700−900 °C	117
Ni		MgO	model syngas, C_6H_6, $C_{10}H_8$	700−900 °C	117
Ni	Ru	MgO	model syngas, C_6H_6, $C_{10}H_8$	700−900 °C	117

Table 6. Fixed- versus Fluidized-Bed Reactor Comparisons

metal	promoter	support	reaction	conditions	references
Ni		Al_2O_3	dry reforming	800 °C	124
Ni		Al_2O_3	dry reforming	750 °C	122
Ni		SiO_2	dry reforming	750 °C	121

such as dolomite and many conventional, high surface area metal oxide supports experience high attrition rates and form many particulates and are therefore unfit for fluidized-bed operation.[3,40]

The use of a fixed "guard bed" reactor, composed of an inexpensive material, such as dolomite, to precondition biomass-derived syngas before it is sent to a fluidized-bed reactor containing a Ni catalyst, has been demonstrated to extend Ni catalyst lifetimes.[125−129] The use of a guard bed helps to reduce the content of tars and impurities, such as sulfur and chlorine, while removing other impurities, such as H_2S.

While a limited number of studies directly compare fluidized- and fixed-bed reactors, the studies indicate that higher activity and lower coking can be achieved with fluidized-bed reactors. Catalyst attrition, however, is a significant barrier limiting the types of catalysts that can realistically be used in a fluidized environment. Catalyst attrition, which is often not measured, must be considered for the development of efficient catalytic syngas conditioning in fluidized reactors. Currently, a combination of fixed guard bed followed by a fluidized-bed reactor represents an attractive option until a suitably stable fluidizable catalyst is discovered.

7. Conclusions

Gasification of lignocellulosic biomass to create syngas for liquid fuel synthesis has the potential to significantly displace petroleum usage. The raw syngas that is currently produced from biomass gasification, however, lacks the necessary quality for fuel synthesis without additional conditioning. While research efforts focused on optimal gasification conditions will be responsible for some improvements in syngas quality, in-bed and/or downstream catalytic conditioning of the syngas will also be necessary. A short syngas conditioning catalyst lifetime is an obstacle currently limiting the thermochemical conversion of biomass to fuels, although recent progress in developing fluidizable reforming catalysts is overcoming this barrier.[8] Other catalyst limitations include (1) coking, (2) sulfur poisoning, (3) attrition, and (4) high cost of materials. Further development of attrition-resistant supports, multimetallic and multifunctional reforming catalysts, and monoliths all hold promise for significant improvements in conditioning biomass-derived syngas. Research efforts to develop catalysts that can overcome each of these barriers will be necessary.

To advance catalytic conditioning technology toward commercialization, further work needs to address extended reforming and regeneration operations in closely modeled or actual biomass-derived syngas to provide the data required to assess eventual use in industrial applications. The current body of work in catalytic syngas conditioning indicates that there is a need to evaluate more catalysts in fluidized-bed reactors in addition to fixed-bed and monolithic reactors. The effects of poisons and trace impurities also need further investigation. In addition to catalyst deactivation by coking and sulfur poisoning, which have not been fully solved, other contaminants present in biomass-derived syngas (e.g., HCl, alkali metals, NH_3, and other inorganics) must be systematically evaluated for their impact on catalyst performance to successfully develop a commercially viable catalytic conditioning system. The effects of these contaminants and also selective sorbents to remove undesired impurities from hot syngas are other suggested research directions.

Acknowledgment. Funding for this work, provided by the U.S. Department of Energy's Biomass Program Contract DE-AC36-99-GO-10337, is gratefully acknowledged.

EF800830N

(125) Caballero, M. A.; Corella, J.; Aznar, M.-P.; Gil, J. *Ind. Eng. Chem. Res.* **2000**, *39*, 1143.
(126) Narváez, I.; Corella, J.; Orío, A. *Ind. Eng. Chem. Res.* **1997**, *36*, 317.
(127) Corella, J.; Aznar, M.-P.; Gil, J.; Caballero, M. A. *Energy Fuels* **1999**, *13*, 1122.
(128) Corella, J.; Orío, A.; Aznar, P. *Ind. Eng. Chem. Res.* **1998**, *37*, 4617.
(129) Corella, J.; Orío, A.; Toledo, J.-M. *Energy Fuels* **1999**, *13*, 702.
(130) Song, H.; Zhang, L.; Watson, R. B.; Braden, D.; Ozkan, U. S. *Catal. Today* **2007**, *129*, 346.
(131) Furusawa, T.; Tsutsumi, A. *Appl. Catal., A* **2005**, *278*, 207.
(132) Furusawa, T.; Tsutsumi, A. *Appl. Catal., A* **2005**, *278*, 195.
(133) Polychronopoulou, K.; Fierro, J. L. G.; Efstathiou, A. M. *J. Catal.* **2004**, *228*, 417.
(134) Corella, J.; Toledo, J. M.; Molina, G. *Bioresour. Technol.* **2008**, *99*, 7539.
(135) Zhang, R.; Wang, Y.; Ma, R.; Wu, D. *Appl. Catal., A* **2003**, *243*, 251.
(136) Natesakhawat, S.; Watson, R.; Wang, X.; Ozkan, U. *J. Catal.* **2005**, *234*, 496.
(137) Li, B.; Kado, S.; Mukainakano, Y.; Miyazawa, T.; Miyao, T.; Naito, S.; Okumura, K.; Kunimori, K.; Tomishige, K. *J. Catal.* **2006**, *245*, 144.
(138) Devi, L.; Ptasinski, K. J.; Janssen, F. J. J. B.; van Paasen, S. V. B.; Bergman, P. C. A.; Kiel, J. H. A. *Renewable Energy* **2005**, *30*, 565.
(139) Wang, T.; Chang, J.; Lv, P; Zhu, J. *Energy Fuels* **2005**, *19*, 22.
(140) Ishihara, A.; Qian, E.; Finahari, I.; Sutrisna, I.; Kabe, T. *Fuel* **2005**, *84*, 1462.
(141) Zhang, R.; Brown, R. C.; Suby, A.; Cummer, K. *Energy Convers. Manage.* **2004**, *45*, 995.
(142) Wang, T. J.; Chang, J.; Wu, C. Z.; Fu, Y.; Chen, Y. *Biomass Bioenergy* **2005**, *28*, 508.
(143) Matsuoka, K.; Shimbori, T.; Kuramoto, K.; Hatano, H.; Suzuki, Y. *Energy Fuels* **2006**, *20*, 2727.
(144) Bona, S.; Guillen, P.; Alcalde, J. G.; Garcia, L.; Bilbao, R. *Chem. Eng. J. (Amsterdam, Neth.)* **2008**, *137*, 587.
(145) Asadullah, M.; Miyazawa, T.; Ito, S.; Kunimori, K.; Tomishige, K. *Energy Fuels* **2003**, *17*, 842.
(146) Tomishige, K.; Miyazawa, T.; Kimura, T.; Kunimori, K. *Catal. Commun.* **2005**, *6*, 37.
(147) Tomishige, K.; Asadullah, M.; Kunimori, K. *Catal. Today* **2004**, *89*, 389.
(148) Asadullah, M.; Miyazawa, T.; Ito, S.-i.; Kunimori, K.; Yamada, M.; Tomishige, K *Appl. Catal., A* **2003**, *255*, 169.
(149) Asadullah, M.; Ito, S.-i.; Kunimori, K.; Yamada, M.; Tomishige, K. *J. Catal.* **2002**, *208*, 255.
(150) Jing, Q.; Lou, H.; Fei, J.; Hou, Z.; Zheng, X. *Int. J. Hydrogen Energy* **2004**, *29*, 1245.
(151) Takeguchi, T.; Kani, Y.; Yano, T.; Kikuchi, R.; Eguchi, K.; Tsujimoto, K.; Uchida, Y.; Ueno, A.; Omoshiki, K.; Aizawa, M. *J. Power Sources* **2002**, *112*, 588.